

Characterization of Radicals Formed Following Enzymatic Reduction of 3-Substituted Analogues of the Hypoxia-Selective Cytotoxin 3-Amino-1,2,4-Benzotriazine 1,4-Dioxide (Tirapazamine)

Sujata S. Shinde,^{†,‡} Andrej Maroz,[†] Michael P. Hay,[‡] Adam V. Patterson,[‡] William A. Denny,[‡] and Robert F. Anderson^{*,†,‡}

Department of Chemistry and Auckland Cancer Society Research Centre, The University of Auckland, Private Bag 92019, Auckland 1142, New Zealand

Received October 12, 2009; E-mail: r.anderson@auckland.ac.nz

Abstract: The mechanism by which the 1,2,4-benzotriazine 1,4-dioxide (BTO) class of bioreductive hypoxia-selective prodrugs (HSPs) form reactive radicals that kill cancer cells has been investigated by steady-state radiolysis, pulse radiolysis (PR), electron paramagnetic resonance (EPR), and density functional theory (DFT) calculations. Tirapazamine (TPZ, 3-amino BTO, **1**) and a series of 3-substituted analogues, -H (**2**), -methyl (**3**), -ethyl (**4**), -methoxy (**5**), -ethoxymethoxy (**6**), and -phenyl (**7**), were reduced in aqueous solution under anaerobic steady-state radiolysis conditions, and their radicals were found to remove the substrates by short chain reactions of different lengths in the presence of formate ions. Multiple carbon-centered radical intermediates, produced upon anaerobic incubation of the compounds with cytochrome P₄₅₀ reductase enriched microsomes, were trapped by *N-tert*-butyl- α -phenylnitron and observed using EPR. The highly oxidizing oxymethyl radical, from compound **5**, was identified, and experimental spectra obtained for compounds **1**, **2**, **3**, and **7** were well simulated after the inclusion of aryl radicals. The identification of a range of oxidizing radicals in the metabolism of the BTO compounds gives a new insight into the mechanism by which these HSPs can cause a wide variety of damage to biological targets such as DNA.

Introduction

Hypoxic cells in tumors are more resistant to both chemotherapy and radiotherapy compared to normoxic cells^{1,2} and are being targeted for selective eradication by the development of hypoxia-selective prodrugs (HSPs).³ The 1,2,4-benzotriazine 1,4-dioxide (BTO) class of HSPs undergo bioactivation⁴ to selectively kill hypoxic cells *in vivo*,^{5–7} with tirapazamine (TPZ, **1**) undergoing extensive clinical trials. TPZ has produced modest therapeutic results⁸ and failed to demonstrate benefit in a recent phase III clinical trial.⁹ Nonetheless, recent prognostic data from a phase II clinical trial in head and neck cancer has highlighted the importance of identifying patients with hypoxia when using

such a targeted therapy.^{10,11} Hypoxic selectivity arises from the susceptibility of the radical anion and its protonated form to back oxidation by molecular oxygen¹² (Scheme 1), preventing formation of a subsequent TPZ-derived radical that reacts to produce DNA strand breaks and the poisoning of topoisomerase II.^{13–16} There have been a number of suggestions as to the identity of this active radical. An early proposal was that the $\cdot\text{OH}$ radical is released from the protonated anion,¹⁷ but this was later rejected in favor of the protonated radical anion itself as being the active species.¹² However, this is a reducing radical that undergoes electron transfer reactions, such as to O₂. Release of an $\cdot\text{OH}$ radical has been favored by other workers, on the basis of the similarity in the spectrum of products arising from TPZ-mediated damage to both purine and pyrimidine bases and deoxyribose sugars, when compared with that arising from the $\cdot\text{OH}$ radical, although TPZ-mediated damage exhibited some

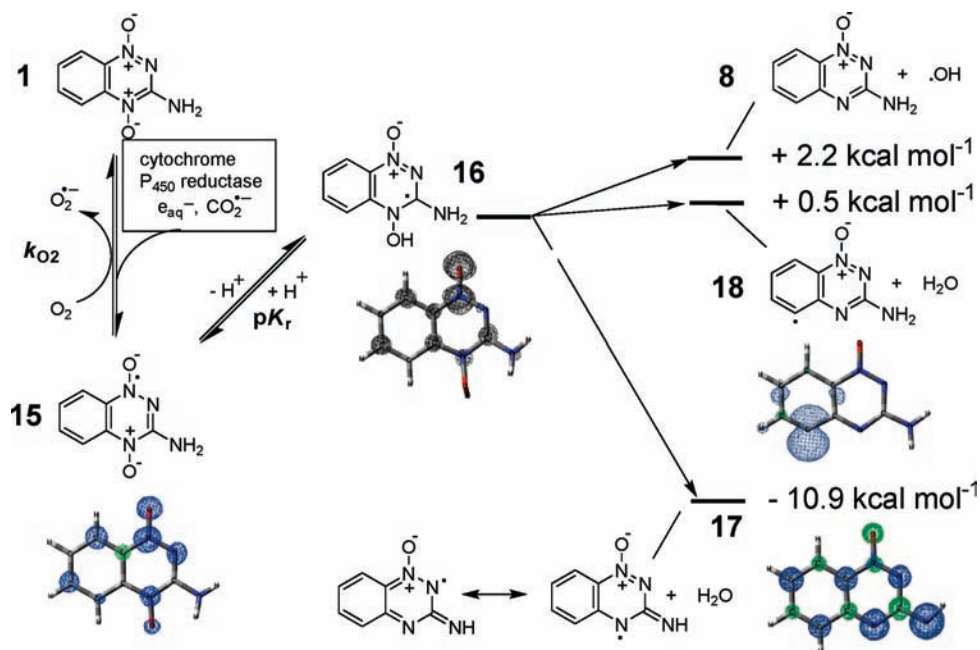
[†] Department of Chemistry.

[‡] Auckland Cancer Society Research Centre.

- (1) Nordmark, M.; Overgaard, M.; Overgaard, J. *Radiother. Oncol.* **1996**, *41*, 31–40.
- (2) Tannock, I. F. *Lancet* **1998**, *351*, SII9–SII16.
- (3) Brown, J. M.; Wilson, W. R. *Nat. Rev. Cancer* **2004**, *4*, 437–447.
- (4) Patterson, A. V.; Saunders, M. P.; Chinje, E. C.; Patterson, L. H.; Stratford, I. J. *Anti-Cancer Drug Des.* **1998**, *13*, 541–573.
- (5) Brown, J. M.; Lemmon, M. J. *Cancer Res.* **1990**, *50*, 7745–7749.
- (6) Brown, J. M.; Lemmon, M. J. *Int. J. Radiat. Oncol. Biol. Phys.* **1991**, *20*, 457–461.
- (7) Dorie, M. J.; Brown, J. M. *Cancer Chemother. Pharmacol.* **1997**, *39*, 361–366.
- (8) Marcu, L.; Olver, I. *Cur. Clin. Pharmacol.* **2006**, *1*, 71–79.
- (9) Rischin, D.; Peters, L.; O'Sullivan, B.; Giralt, J.; Yuen, K.; Trotti, A.; Bernier, J.; Bourhis, J.; Henke, M.; Fisher, R.; Trans-Tasman Radiation Oncology, G. *J. Clin. Oncol. (Meeting Abstr.)* **2008**, *26*, LBA6008.

- (10) Rischin, D.; Fisher, R.; Peters, L.; Corry, J.; Hicks, R. *Int. J. Radiat. Oncol. Biol. Phys.* **2007**, *69*, S61–S63.
- (11) Rischin, D.; Hicks, R. J.; Fisher, R.; Binns, D.; Corry, J.; Porceddu, S.; Peters, L. *J. Clin. Oncol.* **2006**, *24*, 2098–2104.
- (12) Laderoute, K.; Wardman, P.; Rauth, A. M. *Biochem. Pharmacol.* **1988**, *37*, 1487–1495.
- (13) Biedermann, K. A.; Wang, J.; Graham, R. P.; Brown, J. M. *Br. J. Cancer* **1991**, *63*, 358–362.
- (14) Wang, J.; Biedermann, K. A.; Brown, J. M. *Cancer Res.* **1992**, *52*, 4473–4477.
- (15) Peters, K. B.; Brown, J. M. *Cancer Res.* **2002**, *62*, 5248–5253.
- (16) Siim, B. G.; van Zijl, P. L.; Brown, J. M. *Br. J. Cancer* **1996**, *73*, 952–960.
- (17) Laderoute, K. R.; Rauth, A. M. *Biochem. Pharmacol.* **1986**, *35*, 3417–3420.

Scheme 1



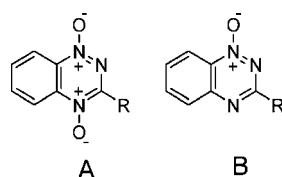
preference for purine damage over pyrimidine damage.^{18–21} Additionally, both an EPR study, using DMPO as a spin trap, which reported a composite spectrum of both a C-centered and an OH-adduct, DMPO-OH,²² and a density functional theory (DFT) study²³ have been quoted as supporting evidence for release of an •OH radical. The DFT study showed that the release of an •OH radical from one-electron reduced TPZ, via the radical anion, is overall endothermic but did not include calculations for other possible pathways. Recently, we have shown that the DMPO-OH EPR spectrum most likely arises from the oxidation of DMPO followed by hydration of the radical cation by the solvent.²⁴ We have also presented UV–vis spectral and kinetic evidence that the protonated radical anion undergoes dehydration to the benzotriazinyl radical (BTZ), which is capable of causing oxidative damage to DNA and to oxidize TPZ itself.^{25–28} In situ EPR measurement²⁴ has confirmed that a multi N-centered radical, consistent with the BTZ radical, is formed when a soluble BTO analogue is reduced by cytochrome P₄₅₀ reductase enriched microsomes in the presence of a high concentration of its 1-oxide. Also, the one-electron reduction potentials of the BTZ radicals, *E*(1)R, track

the hypoxic cytotoxicity to human tumor cells of a series of BTO analogues of TPZ.²⁹ However, although the *E*(1)R value for the BTZ radical of TPZ, 1.31 V,²⁷ is sufficient to oxidize the purine bases of DNA, the *E*(1)R of guanine in the GC base pair of 1.22 V,³⁰ for example, is much less than that required to directly oxidize the pyrimidine bases of DNA, which possess *E*(1)R values of ca. 1.6 V.³¹ Hence, there is interest in identifying other possible radical species formed from BTO compounds, which are stronger oxidants than the BTZ radical.

The enzymatic reduction of 3-methyl-1,2,4-benzotriazine 1,4-dioxide (3) has been recently described as resulting in a spectrum of DNA breakage and base damage similar to that observed for TPZ.³² This analogue, as well as the 3-ethyl (4), 3-methoxy (5), and 3-phenyl (7) analogues of TPZ, have been found to exhibit hypoxic cytotoxicity against human tumor cells comparable to that of TPZ, with the alkyl derivatives being hypoxia-selective.^{33,34} Many other 3-alkyl BTO analogues have hypoxia-selective activity, and a general mode of action *via* an enzymatically released radical or radicals can be inferred for this class of prodrug. The recognition that 3-alkyl BTO compounds act as HSPs, most likely by the same mechanism as does TPZ, opens up the possibility to spin-trap more stable radicals to investigate both the structure and mechanism by which they are formed. In this study we have employed the nitron spin-trap PBN (*N-tert*-butylphenyl- α -nitron) as it can be used to distinguish between adducts arising from different

- (18) Birincioglu, M.; Jaruga, P.; Chowdhury, G.; Rodriguez, H.; Dizdaroglu, M.; Gates, K. S. *J. Am. Chem. Soc.* **2003**, *125*, 11607–11615.
 (19) Chowdhury, G.; Junnotula, V.; Daniels, J. S.; Greenberg, M. M.; Gates, K. S. *J. Am. Chem. Soc.* **2007**, *129*, 12870–12877.
 (20) Daniels, J. S.; Gates, K. S. *J. Am. Chem. Soc.* **1996**, *118*, 3380–3385.
 (21) Kotandeniya, D.; Ganley, B.; Gates, K. S. *Bioorg. Med. Chem. Lett.* **2002**, *12*, 2325–2329.
 (22) Patterson, L. H.; Taiwo, F. A. *Biochem. Pharmacol.* **2000**, *60*, 1933–1935.
 (23) Li, L.-C.; Zha, D.; Zhu, Y.-Q.; Xu, M.-H.; Wong, N.-B. *Chem. Phys. Lett.* **2005**, *408*, 329–334.
 (24) Shinde, S. S.; Hay, M. P.; Patterson, A. V.; Denny, W. A.; Anderson, R. F. *J. Am. Chem. Soc.* **2009**, *131*, 14220–14221.
 (25) Anderson, R. F.; Harris, T. A.; Hay, M. P.; Denny, W. A. *Chem. Res. Toxicol.* **2003**, *16*, 1477–1483.
 (26) Anderson, R. F.; Shinde, S. S.; Hay, M. P.; Denny, W. A. *J. Am. Chem. Soc.* **2006**, *128*, 245–249.
 (27) Anderson, R. F.; Shinde, S. S.; Hay, M. P.; Gamage, S. A.; Denny, W. A. *J. Am. Chem. Soc.* **2003**, *125*, 748–756.
 (28) Shinde, S. S.; Anderson, R. F.; Hay, M. P.; Gamage, S. A.; Denny, W. A. *J. Am. Chem. Soc.* **2004**, *126*, 7865–7874.

- (29) Anderson, R. F.; Shinde, S. S.; Hay, M. P.; Gamage, S. A.; Denny, W. A. *Org. Biomol. Chem.* **2005**, *3*, 2167–2174.
 (30) Shinde, S. S.; Maroz, A.; Hay, M. P.; Anderson, R. F. *J. Am. Chem. Soc.* **2009**, *131*, 5203–5207.
 (31) Steenken, S.; Jovanovic, S. V. *J. Am. Chem. Soc.* **1997**, *119*, 617–618.
 (32) Junnotula, V.; Sarkar, U.; Sinha, S.; Gates, K. S. *J. Am. Chem. Soc.* **2009**, *131*, 1015–1024.
 (33) Hay, M. P.; Pchalek, K.; Pruijn, F. B.; Hicks, K. O.; Siim, B. G.; Anderson, R. F.; Shinde, S. S.; Phillips, V.; Denny, W. A.; Wilson, W. R. *J. Med. Chem.* **2007**, *50*, 6654–6664.
 (34) Kelson, A. B.; McNamara, J. P.; Pandey, A.; Ryan, K. J.; Dorie, M. J.; McAfee, P. A.; Menke, D. R.; Brown, J. M.; Tracy, M. *Anti-Cancer Drug Des.* **1998**, *13*, 575–592.

Table 1. Structures and Physical Chemistry Properties of 3-Substituted BTO Compounds

compd A/B 1,4-dioxide/1-oxide	R	$E(A/A^{\cdot-})$, mV	$E(B/B^{\cdot-})$, mV	$E(B^{\cdot-}, H^+/B)$ \pm 0.01, V	$E(A^{\cdot-}, H^+/A)$ \pm 0.01, V	k_{elim} , s ⁻¹	$10^{-7} 2k$, M ⁻¹ s ⁻¹
1/8	NH ₂	-456 \pm 8 ^a	-568 \pm 8 ^b	1.31 ^d	1.15 ^e	83 \pm 6 ^d	0.62 \pm 0.03
2/9	H	-318 \pm 8	-399 \pm 8	1.34		1428 \pm 63	31.8 \pm 6.5
3/10	CH ₃	-364 \pm 8 ^c	-404 \pm 8	1.33	1.22	11 \pm 4	2.78 \pm 0.16
4/11	CH ₂ CH ₃	-376 \pm 8 ^c	-407 \pm 8	1.33		18 \pm 3	3.14 \pm 0.10
5/12	OCH ₃	-324 \pm 8	-516 \pm 8	1.46	1.20	85 \pm 11	1.30 \pm 0.10
6/13	O(CH ₂) ₂ OCH ₃	-335 \pm 10	-516 \pm 9	1.38		113 \pm 10	1.20 \pm 0.10
7/14	phenyl	-352 \pm 8 ^c	-455 \pm 8	(1.57) ^f	1.34	150 \pm 15	2.20 \pm 0.20

^a From refs 29 and 67. ^b From ref 28. ^c From ref 33. ^d From ref 27. ^e From ref 26. ^f Radical cation of **14**.

Table 2. $G(\text{loss})$ of BTO Compounds (in $\mu\text{M Gy}^{-1}$) and Relative Change in Mass of the Products upon Steady-State Radiolysis in Solution at pH 7.0

compound	formate, N ₂ O-saturated	products, Δ mass, g mol ⁻¹	<i>tert</i> -butanol, deaerated	products, Δ mass, g mol ⁻¹
1	-1.07 \pm 0.07 ^a	-16, ((-32))	-0.18 \pm 0.01 ^a	-16
2	-0.47 \pm 0.01	-16, (-32) ^b	-0.33 \pm 0.02	(no -16 product)
3	-0.44 \pm 0.02	-16, (-32)	-0.13 \pm 0.01	(-16), ((-32))
4	-0.34 \pm 0.02 pH 4			
	-0.34 \pm 0.02 pH 7	-16, -32	-0.14 \pm 0.01	-16, (-32)
5	-3.40 \pm 0.05 pH 5			
	-3.39 \pm 0.15 pH 7	-16, (-32)	-0.29 \pm 0.01	-16, (-32)
	-0.27 \pm 0.01 pH 10			
6	-2.48 \pm 0.20	-16	-0.27 \pm 0.01	-16, (-32)
7	-1.97 \pm 0.50	-16, (-32)	-0.84 \pm 0.16	-16, (-32)

^a From ref 29. ^b Minor product given in parentheses.

C-centered radicals. We identify a number of oxidizing radicals, as well as the likely mechanisms by which they are produced, upon anaerobic reduction by cytochrome P₄₅₀ reductase. A comparison is made between the 3-alkyl BTO compounds that possess α -Hs on the 3-substituent of the BTO (as does TPZ) and analogues that do not. Pulse radiolysis is used to determine redox and kinetic parameters of the initially formed radicals, and steady-state radiolysis is used to investigate the loss of the analogues in the presence of formate ions and 2-methyl-2-propanol for evidence of chain reactions. DFT calculations are performed, in conjunction with EPR experiments, on representative compounds **1**, **2**, **3**, **5**, and **7** to assist in the assignment of the radical species.

Results and Discussion

Pulse Radiolysis Studies. Redox and kinetic parameters for all of the BTO compounds used in this study were determined using pulse radiolysis and are presented in Table 1. The one-electron reduction potentials, $E(1)$, of both the 1,4-dioxides (A) (**1**–**7**) and their 1-oxide, 2-electron-reduced compounds (B) (**8**–**14**), were determined against methylviologen or triquat as the redox standard. All of the analogues tested have the 3-amino substituent of TPZ replaced by less powerful electron-donating substituents, and hence their $E(1)$ values are raised compared to that of TPZ. Similarly, the one-electron reduction potentials of intermediate radicals, $E(1)R$, produced upon one-electron oxidation of the 1-oxides (B) by the SO₄^{•-} or SeO₃^{•-} radicals, were determined against methoxybenzene reference compounds (Experimental Section). The radicals of the 3-alkyl derivatives of TPZ were found to have $E(1)R$ values slightly higher than that of the BTZ radical of TPZ. The $E(1)R$ values for 3-methoxy and 3-ethoxymethoxy derivatives are considerably higher at 1.46

and 1.38 V, respectively. Although a redox equilibrium was established between the 3-phenyl analogue of TPZ and the reference compound, it is unlikely that this is for an aryl radical, as such radicals react by H-atom abstraction rather than by electron transfer. We tentatively propose that the measured $E(1)R$ value of 1.57 V is for the radical cation of **14**. One-electron oxidation of the 3-H analogue **8** most likely forms an aryl-type radical on the 3 position by electron transfer and subsequent loss of the proton at C3, as evidenced by the EPR spectrum using PBN as the spin trap (see below). The decay kinetics of the radical anions of the compounds, formed by electron transfer from the CO₂^{•-} species, were monitored at 500 nm. The kinetic transients decayed with mixed order kinetics and were analyzed to separate out the first order component, $k(\text{elim})$ (associated with the formation of the oxidizing radical), from the second-order decay of the radical anion, $2k(\text{dis})$ (through disproportionation), as previously described.²⁷ While the observed $k(\text{elim})$ values for the radical anions are similar to those found previously for analogues of TPZ of equivalent $E(1)$,²⁹ the radical anion of compound **2** underwent a much faster transformation.

Steady-State Radiolysis Studies. The loss of each BTO 1,4-dioxide compound (50–100 μM), under reducing conditions at pH 7.0, was followed by monitoring the sequential changes in their UV–vis absorption spectra with radiation dose (see Supporting Information, Figure S1, for a representative example) to obtain $G(\text{loss})/\mu\text{M Gy}^{-1}$ ($\mu\text{mol J}^{-1}$) values, which are tabulated in Table 2. Two systems were studied: (i) N₂O-saturated solutions of sodium formate (0.1 M) where $G(\text{CO}_2^{\cdot-})$

= 0.68 $\mu\text{M Gy}^{-1}$ ³⁵ and (ii) deaerated solutions of 2-methyl-2-propanol (0.1 M), where $G(e^-_{\text{aq}}) = 0.28 \mu\text{M Gy}^{-1}$. Previous studies have noted that TPZ is radiolytically removed by a short chain reaction from anaerobic solutions containing formate ions, secondary alcohols, or deoxyribose.^{12,29,36} It has been suggested that part of the observed loss arises from the putative oxidizing radical oxidizing a further BTO molecule.²⁹ The 3-H (**2**) and 3-alkyl BTO compounds (**3**, **4**) gave $G(\text{loss})$ values in formate solution at or slightly greater than one-half of $G(\text{CO}_2^{\cdot-})$ (i.e., $\geq 0.34 \mu\text{M Gy}^{-1}$), with their 1-oxide derivatives being the major product. Whereas the 1-oxide products were observed to be produced upon reduction of compounds **3** and **4** by the e^-_{aq} , in the presence of 2-methyl-2-propanol at half the yield of $G(e^-_{\text{aq}})$, the 1-oxide of compound **2** was not formed, even though $G(\text{loss})$ of **2** equals $G(e^-_{\text{aq}})$. This result implies that a radical–radical reaction likely occurs, either between the radical form of **2** and the 2-methyl-2-hydroxy-1-propyl radical, or possibly its dimerization. The $G(\text{loss})$ results obtained for the 3-OR substituted BTO compounds, **5** and **6**, in solutions containing formate ions are of particular interest. Chain lengths of ca. 5 and 4, respectively, indicate that the active radicals of these compounds can react with formate ions to produce the $\text{CO}_2^{\cdot-}$ species, thus propagating a chain to form their 1-oxide products. However, the fact that the chain reactions are not longer could imply that bifurcation of a precursor radical into two radicals: a radical that can abstract a hydrogen atom from formate ions and another that does not. The contention that these two analogues form highly reactive radicals is supported by the results obtained in the presence of 2-methyl-2-propanol where loss of the compounds equals the full $G(e^-_{\text{aq}})$ yield, implying that the active radicals can abstract an H-atom from the tertiary alcohol. Similar considerations apply to interpreting the results obtained for the 3-phenyl BTO compound (**7**), although the large $G(\text{loss})$ observed in the presence of 2-methyl-2-propanol implies that the active radical itself can propagate a short chain.

EPR Experiments with TPZ (1). The one-electron reduction of TPZ by cytochrome P₄₅₀ reductase enriched microsomes was carried out anaerobically at 37 °C, in situ in an EPR spectrometer, in both pH 7.4 and pH 10.5 solutions. No species were observed in the EPR spectrum at pH 7.4, Figure 1a, in contrast to the earlier reported spectrum obtained using rat liver microsomes.³⁷ Our finding is in agreement with that of other workers who carried out similar experiments using a wide range of protein concentrations and conditions at pH 7.4.²² However, at pH 10.5 we observed a multiline EPR spectrum, Figure 1b. This spectrum is simulated using hyperfine coupling constant (HFC) of $a_{\text{N}} = 11.65 \text{ G}$, $a_{\text{N}'} = 3.62 \text{ G}$, $a_{\text{N}''} = 2.98$, $a_{\text{H}} = 3.05 \text{ G}$ (2), Figure 1c, which corresponds closely to that reported earlier³⁷ and is consistent as arising from the nitroxyl radical positioned on N1, assigned as the radical anion **15** (Scheme 1). The instability of this radical species at pH 7.4 most probably arises from the prototropic property of the radical, $\text{p}K_{\text{a}}$ of 6.2,^{12,27} with the protonated form undergoing rapid transformation and/or bimolecular radical–radical reactions, removing the radical species from solution. When the spin trap PBN was

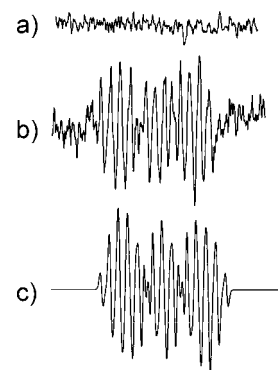


Figure 1. EPR spectra of radicals obtained on enzymatic reduction of **1** (TPZ, 4 mM) by cytochrome P₄₅₀ reductase enriched microsomes (2 mg/mL) of anaerobic solutions containing SOD (250 $\mu\text{g/mL}$), glucose-6-phosphate dehydrogenase (13 units/mL), glucose-6-phosphate (10 mM), and NADPH (1 mM) in the absence of PBN at (a) pH 7.4, (b) pH 10.5, and (c) simulation spectrum of nitroxide radical, **15** ($R = 0.96$).

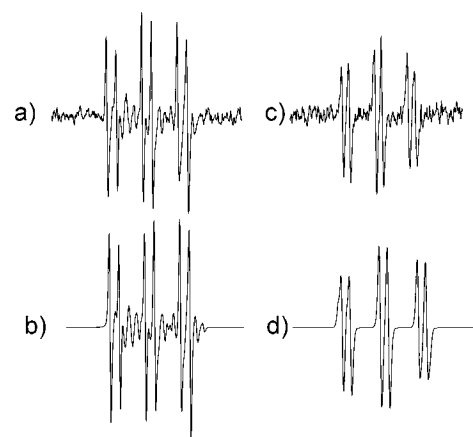


Figure 2. EPR spectra of radicals obtained on enzymatic reduction of **1** (TPZ, 4 mM) under conditions similar to those in Figure 1 in the presence of PBN (50 mM) at (a) pH 10.5 and (c) pH 7.4. Simulation spectrum of PBN-C-R adducts at (b) pH 10.5, with ratio of 0.51: 0.49 for radicals **18**: **15** ($R = 0.96$) and (d) pH 7.4, with ratio of 0.80: 0.20 for radicals **16**:**18** ($R = 0.96$).

added to the incubation mixture, the EPR spectrum at pH 10.5 changed to a doublet of triplets typical of a PBN-carbon radical adduct and additional lines superimposed in the center of the spectrum, Figure 2a. This spectrum could be simulated by the presence of two species, **15** and **18**, in the ratio 0.49:0.51, Figure 2b and Tables 3 and 4. The large HFC for the β -hydrogen, relative to the location of the unpaired spin on the spin trap, a_{H^β} , of 4.18 G is indicative of an aryl-type radical and is tentatively assigned to the PBN-adduct of species **18**, Table 4. Formation of such a species would imply that the hydrogen at C5 is lost in the dehydration of the radical anion. The rate constant for the elimination of water from the radical anion decreases with increasing pH above the $\text{p}K_{\text{a}}$ of the radical and can be calculated²⁹ as 0.015 s^{-1} at pH 10.5. The lifetime of the resulting trapped radical species (ca. 20 min) at this pH is long enough for a steady-state concentration to be formed and detected by EPR. At pH 7.4, a typical C-centered radical spectrum was observed with PBN, Figure 2c. This spectrum could arise from trapping of the protonated radical anion **16** (which possesses some spin density on the C3 position in contrast to **15**, Scheme 1) or, as others have speculated, from C-centered radicals arising from the putative, TPZ-derived oxidizing radical, reacting with materials in the biological

(35) Mulazzani, Q. G.; Venturi, M.; Hoffman, M. Z.; Rodgers, M. A. J. *J. Phys. Chem.* **1986**, *90*, 5347–5352.

(36) Wardman, P.; Dennis, M. F.; Everett, S. A.; Patel, K. B.; Stratford, M. R. L.; Tracy, M. In *Free Radicals and Oxidative Stress: Environment, Drugs and Food Additives*; Rice-Evans, C. A., Halliwell, B., Lund, G. G., Eds.; Portland Press: London, 1995; Vol. 61, pp 171–194.

(37) Lloyd, R. V.; Duling, D. R.; Rummyantseva, G. V.; Mason, R. P.; Bridson, P. K. *Mol. Pharmacol.* **1991**, *40*, 440–445.

Table 3. Hyperfine Coupling Constants in Gauss Measured for Radical Species Trapped by PBN

compound	radical	a_N	a_H^β	a_H^γ
1 (3-NH ₂ , TPZ)	16	16.18	3.45	
	18	16.50	4.18	
2 (3-H)	19	16.75	3.67	1.05
	20	15.90	4.98	
3 (3-CH ₃)	22	<i>15.4^a</i>	<i>3.06^a</i>	
	23	15.64	3.83	0.96
	24	15.96	4.31	
5 (3-OCH ₃)	25	15.19 ^b	3.51 ^b	
	26	16.20	3.77	1.09
	27	nd ^c		
7 (3-phenyl)	28	16.18	3.66	
	29	16.21	4.18	

^a Values in italics obtained from simulation spectrum. ^b Measured at 15 °C. ^c nd: not detected.

matrix. The lack of additional splitting, which would be expected for C-centered radicals bearing one or more γ -hydrogens relative to the location of spin on the spin trap, favors this assignment as **16** trapped at the C3 position. However, simulation of this spectrum indicates the presence of the two species, a C-centered radical, **16**, and an aryl-type radical, **18**, in the ratio 0.80:0.20, Figure 2d. The minor species decayed away faster (within 1 h) than the major species, which was stable for up to 3 h. Varying the concentration of PBN from 25 to 100 mM did not change the ratio of the two trapped species but increased the intensity of the measured spectra. In addition, we carried out similar experiments using the 5-methoxy substituted analogue of TPZ (see Supporting Information, Figure S3) and observed a PBN-carbon radical adduct spectrum, without a large HFC of a_H^β as tentatively assigned to the aryl-type radical above but with that for a typical carbon radical adduct with values of $a_N = 16.02$ G and $a_H^\beta = 3.70$ G. It should be noted that, under the conditions used, PBN did not successfully trap the N-centered BTZ radical of TPZ (**17**). This species is also formed by a dehydration reaction involving an α -hydrogen on the 3-amino substituent of BTO radicals, but could only be trapped for an analogue when a large excess of its BTO 1-oxide was also present.²⁴

DFT Calculations for TPZ-Derived Radicals. Possible fates of the protonated radical anion of TPZ, **16**, were investigated by calculating the differences in overall energy for three elimination pathways leading to different radical intermediates (Scheme 1): (i) homolytic fragmentation to the 1-oxide (**8**) with the release of the \cdot OH radical is calculated to be endothermic, (ii) elimination of a water molecule to give the aryl radical centered at C5, radical **18**, does not result in an overall change in energy (within calculation error) and, (iii) the elimination of a water molecule to give the BTZ radical **17** is strongly exothermic.

EPR Experiments with 3-Substituted BTO Compounds. The one-electron reduction of a series of representative compounds **2**, **3**, **5**, and **7** by cytochrome P₄₅₀ reductase enriched microsomes was carried out anaerobically at 37 °C in situ in an EPR spectrometer in the presence of PBN. EPR spectra of radical intermediates trapped by PBN are presented in Figures 3 and 4. The EPR spectrum obtained using compound **2** (3-H BTO) as the substrate, Figure 3a, shows a doublet of triplets indicative of a PBN-carbon centered radical adduct with a wide splitting of the HFC for the β -hydrogen, relative to the location of the unpaired spin on the spin trap, a_H^β . This spectrum could be simulated with an excellent fit by combining two species, (i) **20** and (ii) **19** (Table 3), in the ratio of 0.92:0.08, Figure 3b. The large a_H^β value for species (i) is indicative of an aryl type

radical or possibly an α -aminoalkyl radical. The HFC is greater than that typically found for an aryl radical (a_H^β ca. 4.1–4.3 G)^{38–40} but can be assigned to the radical **20** rather than radical **21** (see Table 4) on the grounds that the unpaired electron is adjacent to a nitrogen atom resulting in conjugative delocalization.⁴¹ Minor species (ii) most likely arises from trapping of the protonated radical anion, **19**, which accounts for the observed small γ -hydrogen splitting, relative to the location of the spin on the spin trap arising from the hydrogen on C3 of the BTO compound. Incubation of compound **7** (3-phenyl BTO) resulted in a spectrum, Figure 3c, which is closely simulated by the presence of three PBN-carbon-centered radical adducts, all without additional splitting in the ratio 0.66:0.26:0.08. Comparing the HFC values of a_H^β for the aryl radicals of TPZ and compound **3** (below) enables assignment of the major radical species as an aryl radical, most likely radical **29** on the basis of DFT calculations, to be made. The obtained spectrum is best simulated by including two trapped C-centered radicals with HFC values of $a_N = 15.59$ G, $a_H = 3.71$ G and $a_N = 15.75$ G, $a_H = 3.68$, in addition to an aryl radical (**29**) of HFC $a_N = 16.27$ G, $a_H = 4.20$ G, Figure 3d. These two species (in the ratio 0.26:0.08) differ in their a_N parameter and may indicate that radical **28** can be trapped by PBN in two forms, one of which could be protonated on nitrogen. Incubation of compound **3** (3-CH₃ BTO) resulted in an asymmetric 6-line spectrum with wide line separations and some additional splitting, Figure 4a, which indicates the presence of multiple species: (i) the 3-methyl radical (3-CH₂ \cdot), **23**, identified by additional splitting due to the two equivalent γ -hydrogens, relative to the location of the spin on the spin trap and (ii) aryl radical **24**, giving rise to a large a_H value, Tables 3 and 4. Simulation indicated the presence of radicals **23** and **24** in the ratio 0.55:0.31 that formed the major part of a simulation, Figure 4b. The inclusion of a third species, with HFC values of $a_N = 15.41$ G and $a_H^\beta = 3.06$ G and ratio of 0.14, improved the simulation, resulting in a better correlation coefficient. Although the a_H^β value is smaller than expected for a PBN-carbon centered radical adduct (3.4–3.7 G), it can possibly be assigned to radical **22** on the basis that the -CH₃ group attached to the radical site at 3C probably influences the dihedral angle of the β -hydrogen on the spin trap to result in a lower value. For compound **5** (3-OCH₃ BTO), an asymmetric spectrum was also observed, Figure 4c, indicating the presence of more than one species. The spectrum could be simulated by the presence of (i) the oxymethyl radical (-OCH₂ \cdot) **26** and (ii) a radical, tentatively assigned to the protonated anion **25**, in the ratio 0.62:0.38, Figure 4d. Support for these assignments come from the observed (i) additional splitting due to the two equivalent γ -hydrogens, relative to the location of spin on the spin trap, of the 3-OCH₂ \cdot radical and no additional splitting for (ii). Lowering the temperature to 15 °C resulted in a spectrum with improved resolution (dotted spectrum Figure 4c). No evidence was found for the formation of an aryl-type radical, radical **27** upon the reduction of compound **5**.

DFT Calculations for Radicals Arising from 3-Substituted BTO Compounds. Calculations of the relative changes in free energy to form radical intermediates from their precursor protonated radical anions by different pathways, together with

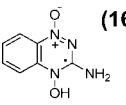
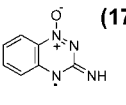
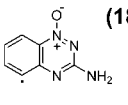
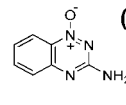
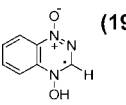
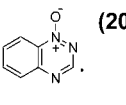
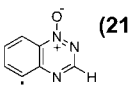
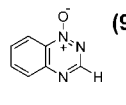
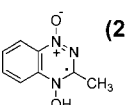
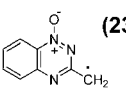
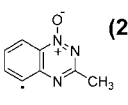
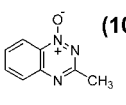
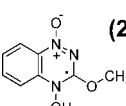
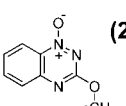
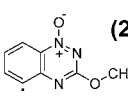
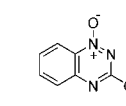
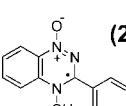
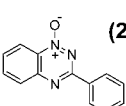
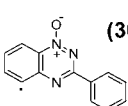
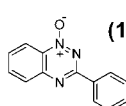
(38) Buettner, G. R. *Free Radical Biol. Med.* **1987**, *3*, 259–303.

(39) Hill, H. A. O.; Thornalley, P. J. *Biochim. Biophys. Acta* **1983**, *762*, 44–51.

(40) Janzen, E. G.; Coulter, G. A.; Oehler, U. M.; Bergsma, J. P. *Can. J. Chem.* **1982**, *60*, 2725–2733.

(41) Grover, T. A.; Ramseyer, J. A.; Piette, L. H. *Free Radical Biol. Med.* **1987**, *3*, 27–32.

Table 4. DFT Calculations for Change in Energy (kcal mol⁻¹) for the Formation of Different Radical Species from the Protonated Radical Anions of the Compounds

Compound	Protonated Radical Anion	Water elimination		•OH elimination
		Radical on 3-substituent	Aryl radical at C5	
1	 (16)	 (17)	 (18)	 (8)
		-10.9	+0.5	+2.2
2	 (19)	 (20)	 (21)	 (9)
		-1.7	+4.6	+5.9
3	 (22)	 (23)	 (24)	 (10)
		-19.4 (-20.0) ^a	+4.0 (+4.4) ^a	+5.5 (+6.7) ^a
5	 (25)	 (26)	 (27)	 (12)
		-14.5	+3.2	+4.5
7	 (28)	 (29)	 (30)	 (14)
		-1.7	0.0	+1.6

^a Values in parentheses are for taking into account solvent effects; see text.

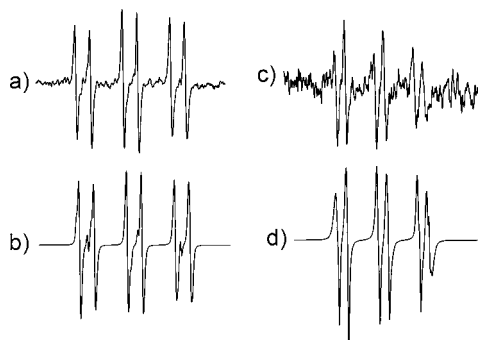


Figure 3. EPR spectra of radicals obtained on enzymatic reduction of BTO compounds under conditions similar to those in Figure 1 at pH 7.4 in the presence of PBN (50 mM): (a) **2** (3-H BTO, 5 mM) and (c) **7** (3-phenyl BTO, 1.4 mM). Simulation spectrum of PBN-C-R adducts obtained for (b) **2** (3-H BTO) with ratio of 0.92:0.08 for radicals **20:19** ($R = 0.99$) and (d) **7** (3-phenyl BTO) with ratio of 0.66:0.26:0.08 for radicals **30** and **28** (plus an unidentified radical) ($R = 0.93$).

calculations on the spin distribution on the initially formed protonated radical anion and other radical intermediates, were performed for compounds **2**, **3**, **5**, and **7**. Full listings of these data obtained are given in Supporting Information, and the overall results, together with data for TPZ, are tabulated in Table 4. In all cases, homolytic fragmentation to the 1-oxides and release of the •OH radical is endothermic. Calculations for radical **19** (from compound **2**) show that the elimination pathway

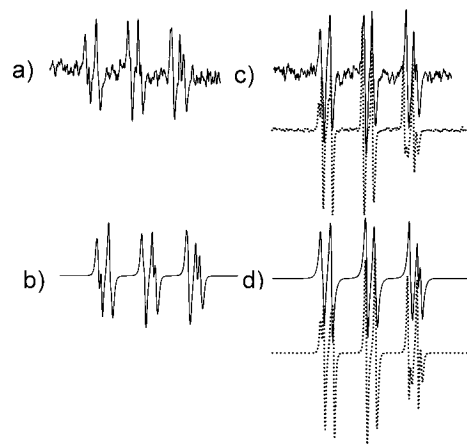


Figure 4. EPR spectra of radicals obtained on enzymatic reduction of BTO compounds under conditions similar to those in Figure 1 at pH 7.4 in the presence of PBN: (a) **3** (3-CH₃ BTO, 6 mM) and (c) **5**, (3-OCH₃ BTO, 5 mM). Simulation spectrum of PBN-C-R adducts obtained for (b) **3** (3-CH₃ BTO) with ratio of 0.55:0.31:0.14 for radicals **23:24:22** ($R = 0.95$) and (d) **5** (3-OCH₃ BTO) with ratio of 0.62:0.38 for radicals **26:25** ($R = 0.98$), dotted line spectrum in (c) and (d) at 15 °C.

to give aryl radical **21** is also endothermic, whereas formation of aryl-type radical **20** is exothermic and serves to support the EPR assignment made above. Calculations for radical **22** (from compound **3**) reveal that formation of the (3-CH₂•), radical is strongly exothermic, compared to the formation of the aryl

radical **24**, Table 4. It should be noted that all calculations are performed for the gas phase, as we find that the use of the IEFPCM solvation model, using radical **22** (from compound **3**), for example, does not significantly affect the results (Scheme S2, values in parentheses, Supporting Information). This is to be expected, as there are no charged species involved in the mechanism. Calculations for radical **25** (from compound **5**) show that the elimination of a water molecule to give the aryl radical centered on C5 (**27**) is endothermic, whereas the elimination of a water molecule to give the triazinomethyl radical (**26**) is strongly exothermic. Formation of this radical is only favorable when the methyl moiety is aligned with the protonated 4-NOH axis. Despite this configuration not being a minimum, the unhindered rotation of -OCH₃ fully allows for it. The above EPR result indicates that the triazinomethyl radical (**26**) is one of the major species formed. Calculations for radical **28** (from compound **7**) show that the elimination of water to give rise to the aryl radical **30** centered on C5 is without change in the overall energy, whereas formation of the phenyl radical **29** on the 3-substituent is slightly exothermic.

Conclusions

The results from this and our recently reported study²⁴ indicate that, following one-electron reduction of the 3-substituted BTO compounds, the initial radical intermediates undergo a variety of transformation reactions that are dependent on the nature of the substituent. It is suggested that the mechanism by which these transformations take place, to form trappable intermediates, is by water elimination from the protonated radical anion. Loss of water effectively changes the redox state of the radical intermediates from reductants to oxidants through redistribution of the unpaired electron density, which can take a number of different forms dependent on the nature of the 3-substituent. DFT calculations show that the formation of the BTZ radical **17** is most favorable upon reduction of TPZ at pH 7.4 and is entirely consistent with our original evidence-based proposal.^{27,29} Such calculations are done in a nondynamic sense and cannot be always directly related to the observations made using spin traps and EPR. The effective scavenging of radical **16**, for example, would prevent the possible formation of radical **17**. However, the evidence obtained at high pH points to some formation of an aryl radical, and this species is also simulated to be a minor species formed at pH 7.4. The suggested aryl radicals formed upon reduction of the 3-methyl and 3-phenyl analogues were sufficiently stable to be trapped and simulated in higher proportions at pH 7.4 than for TPZ. We are unaware of precedents in the literature for the proposed dehydration reaction from the protonated *N*-oxide moiety involving the neighboring hydrogen on C5 as in radical **16**. However there are examples in the literature for the transition from π - to σ -radicals upon the fragmentation of N–O bonds in substituted pyridinium compounds. The supporting theory points to the importance of the orbital mixing allowed by the N–O bond being out of plane with the aromatic ring.⁴² In our case, the protonated radical for TPZ, **16**, has a calculated out of plane N1–N4–O angle of 162° (see Supporting Information, Figure S4), which could allow for a mixing of π^* and σ^* orbitals required for bond fragmentation. Indirect evidence for the proposed generation of the C5-aryl radical, **18**, can be taken from the reported formation of the C5-methyl adduct of TPZ

upon exposure of TPZ to methyl radicals.⁴³ An alternative initiating reaction to that proposed by these authors of the methyl radical addition to the C5 position is for methyl radical addition to the oxygen of the N–O bond. There is both experimental and theoretical evidence for this reaction between TPZ and C-centered radicals.^{44,45} Such a reaction would produce a radical species similar to **16**, which upon the elimination of methanol produces the C5-aryl radical, which could undergo a radical–radical reaction with a further methyl radical to form the product. Furthermore, methoxy substitution on the 5-position of TPZ eliminates the need to include an aryl radical in the simulation (see Supporting Information). This observation strengthens our proposal that the aryl radical at C5 possibly arises from a dehydration reaction of the radical anion of TPZ that involves the C5 hydrogen. Such aryl radicals are best described as phenyl-type radicals, which are known to react with purine and pyrimidine bases, cleave DNA nonspecifically, and be inhibited by hydrogen donors such as ethanol and thiol compounds.^{46,47} In addition, phenyl radicals *in vitro* are known to abstract an H-atom from added formate ions to form the reducing carbon dioxide radical anion,^{48,49} which can then reduce electron-affinic compounds. Such a series of reactions may explain the observed removal of the BTO compounds from solution by chain reactions, with the shortness of the chain arising from bifurcation of the precursor radical into a phenyl radical and another radical species (i.e., in the case of TPZ, the BTZ radical **17**) that does not abstract H-atoms from formate ions or alcohols. The aryl radical formed for the 3-H analogue, compound **2**, with the radical center positioned between two nitrogens on the triazine ring, does not induce a chain reaction in the presence of formate ions, such as that seen for compound **7**. This observation may possibly be due to radical **20** being unable to abstract H-atoms from formate ions.

Although DFT calculations for several of the 3-substituted BTO compounds indicate that the elimination of an $\cdot\text{OH}$ radical from the protonated radical anions is less favorable than formation of their aryl radicals, the difference in overall energy between the two reaction pathways is small. However, we could not find any evidence that the $\cdot\text{OH}$ radical is eliminated from TPZ following enzymatic reduction.²⁴ One-electron transfer from photoexcited dyes is known to release alkoxy radicals from *N*-alkoxy-pyridinium compounds in organic solvents,^{42,50} and to release the $\cdot\text{OH}$ radical from *N*-hydroxypyridine-2(1H)-thione in both organic^{51,52} and aqueous solvents.^{53,54} The nonphotolytic release of an $\cdot\text{OH}$ radical from one-electron reduced organic compounds in aqueous solution, as modeled

(42) Lorange, E. D.; Kramer, W. H.; Gould, I. R. *J. Am. Chem. Soc.* **2002**, *124*, 15225–15238.

(43) Fuchs, T.; Barnes, C. L.; Gates, K. S. *J. Chem. Crystallogr.* **2001**, *31*, 387–391.

(44) Ban, F.; Gauld, J. W.; Boyd, R. J. *J. Am. Chem. Soc.* **2001**, *123*, 7320–7325.

(45) Hwang, J.-T.; Greenberg, M. M.; Fuchs, T.; Gates, K. S. *Biochemistry* **1999**, *38*, 14248–14255.

(46) Griffiths, J.; Murphy, J. A. *J. Chem. Soc. Commun.* **1992**, 24–26.

(47) Hiramoto, K.; Kaku, M.; Kato, T.; Kikugawa, K. *Chem.-Biol. Interact.* **1995**, *94*, 21–36.

(48) Matasović, B.; Bonifačić, M. *J. Phys. Chem. A* **2007**, *111*, 8622–8628.

(49) Packer, J. E.; Heighway, C. J.; Miller, H. M.; Dobson, B. C. *Aust. J. Chem.* **1980**, *33*, 965–977.

(50) Gould, I. R.; Shukla, D.; Giesen, D.; Farid, S. *Helv. Chim. Acta* **2001**, *84*, 2796–2812.

(51) Barton, D. H. R.; Jaszberenyi, J. C.; Morrell, A. I. *Tetrahedron Lett.* **1991**, *32*, 311–314.

(52) Boivin, J.; Crépon, E.; Zard, S. Z. *Tetrahedron Lett.* **1990**, *31*, 6869–6872.

(53) Hess, K. M.; Dix, T. A. *Anal. Biochem.* **1992**, *206*, 309–314.

(54) Reszka, K. J.; Chignell, C. F. *Photochem. Photobiol.* **1995**, *61*, 269–275.

by the scavenging of the e_{aq}^- species is unknown, except for the splitting of the O–O bond in H_2O_2 .⁵⁵ Reduction of the 3-methoxy analogue results in the formation of the oxymethyl radical ($3-OCH_2\cdot$) without the need to include an aryl radical in the simulation. We have determined the one-electron reduction potential of this species, $E(1R)$, to be 1.46 V, which in view of the observed chain reaction for the removal of substrate, is also likely to abstract a H-atom from formate ions. The discovery of the possible involvement of aryl radicals in the cytotoxicity of TPZ is of particular note, as such radicals are highly reactive and are being studied for their possible cytotoxic effects, for example, in the case of amiodarone in causing pulmonary toxicity.^{56,57}

The results from our studies may be able to provide a satisfactory explanation as to why TPZ and compound **3** are reported to significantly effect a larger amount of purine base damage over pyrimidine base damage in duplex DNA.^{18,32} This most likely arises because the BTZ radical, **17**, and radical **23** are produced, which have some specificity for reaction with purine bases, as well as the proposed aryl radicals **18** and **24**, which react with both pyrimidine and purine bases. Hydroxylation of DNA bases is then caused by BTO parent compounds through (i) radicals **17** and **23** preferentially oxidizing purine bases to their radical cations followed by reaction with water, and (ii) the aryl radicals **18** and **24**, abstracting H-atoms from both purine and pyrimidine bases followed by transient adduct formation on the N-oxide moiety of a second molecule with the base radical. Such adducts may break down, either via cation formation or N–O homolysis, to yield hydroxylated products, in a way similar to that known for nitroaromatic and N-oxide compounds reacting with DNA sugar radicals.^{45,58}

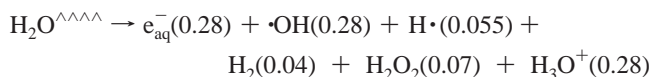
The identification of the range in radical intermediates produced upon the enzymatic reduction of TPZ and BTO analogues now opens up studies to ascertain their properties and reactivity toward target molecules such as DNA as a mechanistic approach to improving this class of anticancer agents.

Experimental Section

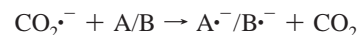
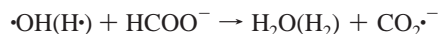
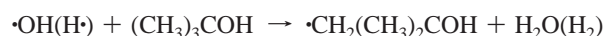
Materials. TPZ (**1**) and the corresponding 1-oxide (**8**) were synthesized as previously described.⁵⁹ Compounds **3**, **4**, **5**, **7**, **10**, **11**, **12**, and **14** were synthesized as previously described.³³ The synthesis of oxides **2**, **6**, **9**, and **13** are described in Supporting Information. Other chemicals were obtained from Sigma, with the exceptions of the spin trap, *N*-tert-butyl- α -phenylnitron (PBN), which was obtained from Fluka, and NADPH (β -nicotinamide adenine dinucleotide phosphate) from Applichem. Cytochrome P450 reductase enriched microsomes⁶⁰ were prepared as described.²⁴

Radiation Chemistry. Time-resolved optical absorption and kinetic studies were carried out using a 4 MeV linear accelerator which delivered 200 ns electron pulses of typically 2.5 Gy dose. The optical detection system and method of dosimetry have been

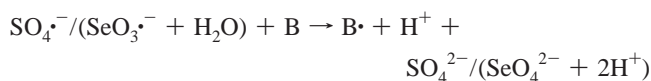
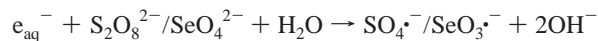
described.⁶¹ The radiolysis of water produces three well-characterized reactive radical species used to initiate radical reactions, as well as molecular products (μM per absorbed dose of 1 Gy ($J\ kg^{-1}$) given in parentheses).



One electron reductions of the benzotriazine 1,4-dioxides and 1-oxides (A/B) were carried out by (i) the e_{aq}^- , while at the same time scavenging the oxidizing radicals with 2-methylpropan-2-ol to form an inert radical, and (ii) electron transfer from the $CO_2\cdot^-$ species ($E^0\ CO_2/CO_2\cdot^- = -1.90\ V^{62}$) in N_2O -saturated solutions (to quantitatively convert the e_{aq}^- to $\cdot OH$ radicals) containing 0.1 M sodium formate, to convert the $\cdot OH$ radicals and H-atoms to $CO_2\cdot^-$.



One-electron oxidation of the benzotriazine 1-oxides (B) was carried out by reaction with the sulfate radical ($SO_4\cdot^-$) or selenite radical ($SeO_3\cdot^-$) produced on scavenging the e_{aq}^- by reaction with sodium peroxidodisulfate or sodium selenate (25 mM) in deaerated solutions containing 2-methylpropan-2-ol (0.2 M) to scavenge the $\cdot OH$ radicals.



The one-electron reduction potentials of the compounds, $E(A/A\cdot^-)$ and $E(B/B\cdot^-)$, versus NHE, were determined at pH 7.0 (5 mM phosphate buffer) by establishing redox equilibria between three mixtures of the one-electron reduced compounds and the reference compounds methylviologen ($E(MV^{2+}/MV^{\cdot+}) = -447 \pm 7\ mV$) or triquat ($E(TQ^{2+}/TQ^{\cdot+}) = -548 \pm 7\ mV$) and calculating ΔE values from the equilibrium constants, K_e , using the Nernst equation, as described in the literature.⁶³ Similarly, the one-electron reduction potentials of the benzotriazinyl and related radicals, $E(B\cdot, H^+/B)$, and of the 1,4-dioxides, $E(A\cdot, H^+/A)$, were determined between mixtures of the oxidized benzotriazine 1-oxides or benzotriazine 1,4-dioxides and the reference compounds 1,2,4-trimethoxybenzene, $E(1,2,4-TMB\cdot^+/TMB) = 1.13 \pm 0.02\ V$; 1,4-dimethoxybenzene, $E(1,4-DMB\cdot^+/1,4-DMB) = 1.30 \pm 0.02\ V$; 1,2-dimethoxybenzene, $E(1,2-DMB\cdot^+/1,2-DMB) = 1.44 \pm 0.02\ V$; or 1,3-dimethoxybenzene $E(1,3-DMB\cdot^+/1,3-DMB) = 1.60 \pm 0.02\ V$.⁶⁴

(61) Anderson, R. F.; Denny, W. A.; Li, W.; Packer, J. E.; Tercel, M.; Wilson, W. R. *J. Phys. Chem. A* **1997**, *101*, 9704–9709.

(62) Schwarz, H. A.; Dodson, R. W. *J. Phys. Chem.* **1989**, *93*, 409–414.

(63) Wardman, P. *J. Phys. Chem. Ref. Data* **1989**, *18*, 1637–1755.

(64) Jonsson, M.; Lind, J.; Reitberger, T.; Eriksen, T. E.; Merényi, G. *J. Phys. Chem.* **1993**, *97*, 11278–11282.

(55) Currie, D. J.; Dainton, F. S. *Trans. Faraday Soc.* **1965**, *61*, 1156–1165.

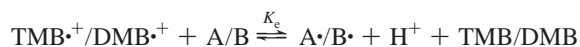
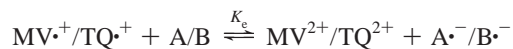
(56) Nicolescu, A. C.; Comeau, J. L.; Hill, B. C.; Bedard, L. L.; Takahashi, T.; Brien, J. F.; Racz, W. J.; Massey, T. E. *Toxicol. Appl. Pharmacol.* **2007**, *220*, 60–71.

(57) Vereckei, A.; Blazovics, A.; Gyorgy, I.; Feher, E.; Toth, M.; Szenasi, G.; Zsinka, A.; Foldiak, G.; Feher, J. *J. Cardiovasc. Electrophysiol.* **1993**, *4*, 161–177.

(58) Kappen, L. S.; Lee, T. R.; Yang, C.-C.; Goldberg, I. H. *Biochemistry* **1989**, *28*, 4540–4542.

(59) Mason, J. C.; Tennant, G. *J. Chem. Soc. B* **1970**, 911–916.

(60) Cowen, R. L.; Patterson, A. V.; Telfer, B. A.; Airley, R.; Hobbs, S.; Philips, R. M.; Jaffar, M.; Stratford, I. J.; Williams, K. J. *Mol. Cancer Ther.* **2003**, *2*, 901–909.



Steady-state radiolysis experiments to determine $G(\text{loss})$ values for the compounds, were performed using a ^{60}Co γ -source delivering a dose rate of ca. 6 Gy min^{-1} , as previously described.²⁹

Methodology for EPR Study. EPR experiments were carried out within a TE₀₁₁ cavity on a JEOL (JES-FA-200) EPR spectrometer, equipped with a variable temperature controller (ES-DVT4) and operated at a 9.1 GHz and 100 kHz field modulation.

All solutions were prepared in Milli-Q water pretreated with Chelex-100 resin to remove trace amounts of polyvalent metal ions, and diethylenetriaminepentaacetic acid (DTPAC) ($100 \mu\text{M}$) was added to the solutions to suppress Fenton-type chemistry. Aqueous solutions of TPZ and analogues (in phosphate buffer, 50 mM at pH 7.4), NADPH, and PBN were predegassed separately with N_2 gas. Superoxide dismutase from bovine erythrocytes (SOD), glucose-6-phosphate (G-6-P), glucose-6-phosphate dehydrogenase (G-6-P-D), cytochrome P₄₅₀ reductase enriched microsomes, and the spin traps, were added into the sample vial under N_2 atmosphere. G-6-P and G-6-P-D were added to the solutions to regenerate NADPH, a cofactor for cytochrome P₄₅₀ reductase enzyme. All additions were carried out on ice, and the enzyme reaction was started by the addition of NADPH. Solutions were adjusted to basic pH by addition of 1 M sodium hydroxide. An EPR flat quartz cell, designed for the variable temperature dewar, was used for all measurements. Solutions for EPR measurements were transferred under N_2 from the sample vial to the EPR cell, which had been flushed previously with N_2 , and inserted into the EPR cavity. Extreme care was taken to keep the system deaerated at all times. The temperature of the cavity was raised to $37 \text{ }^\circ\text{C}$ to activate the enzyme incubation. EPR spectra were monitored as the reaction

progressed, and scans were averaged to improve the signal-to-noise ratio. EPR spectra, recorded at a power of 20 mW, were averaged (5–10 scans) over a scan range of 200 G at a modulation width of 0.5 G, scan time of 2 min, and time constant of 0.1 ms. Computer simulation of spectra were carried out using the WINSIM EPR program available in the public domain of the NIEHS EPR database. The correlation coefficient, R , for all the spectral simulations was ≥ 0.93 .

Density Functional Theory Calculations. DFT calculations were carried out using the Gaussian 03 revision C.02 software package.⁶⁵ The unrestricted nonlocal B3LYP functional hybrid method with the 6-311+G(d,p) basis set was employed throughout. Zero point energy scaling was performed using the scaling factor of 0.9877.⁶⁶ Integral equation formalism PCM (IEFPCM) model was utilized to predict the solvation effect (with water as a solvent). Self consistent field (SCF) spin density distribution is used for visualization purposes in Scheme 1 (isovalue = 0.005).

Acknowledgment. This work was supported by Grant 07/243 from the Health Research Council of New Zealand.

Supporting Information Available: Synthesis details, an example UV–vis spectra with $G(\text{loss})$ analysis, EPR control experiments and EPR study with 5-methoxy TPZ, DFT derived energy diagrams, full citation for ref 65, and optimized geometry for protonated radical anion for N1–N4–O angle. This material is available free of charge via the Internet at <http://pubs.acs.org>.

JA908689F

(65) Frisch, M. J. et al. *Gaussian 03, revision C.02*; Gaussian, Inc.: Wallingford, CT, 2004.

(66) Andersson, M. P.; Uvdal, P. *J. Phys. Chem. A* **2005**, *109*, 2937–2941.

(67) Priyadarsini, K. I.; Tracy, M.; Wardman, P. *Free Radical Res.* **1996**, *25*, 393–400.